Universiteit
Leiden
The Netherlands

Glycosyl cations in glycosylation reactions

Hansen, T.

Citation
Hansen, T. (2020, November 25). *Glycosyl cations in glycosylation reactions*. Retrieved from https://hdl.handle.net/1887/138249

Version:	Publisher's Version
License:	Licence agreement concerning inclusion of doctoral thesis in the Institutional Repository of the University of Leiden
Downloaded from:	https://hdl.handle.net/1887/138249

Note: To cite this publication please use the final published version (if applicable).

Chapter 1

General Introduction

Carbohydrates and glycoconjugates are the most diverse and abundant class of biomolecules occurring in all kingdoms of life. They are involved in a significant number of pathologies, including bacterial infections, cancer, and inflammatory diseases.[1] They fulfill an indispensable role as structural components, in energy housekeeping, and as signaling molecules. The study of carbohydrates and the development of carbohydrate-based medication (*e.g.*, antibacterials, anticancer agents, and vaccines) has been challenging because these molecules are often present in nature as heterogenic mixtures, which complicates their isolation from these sources.

Synthetic chemistry is one of the most important suppliers of well-defined and single molecule carbohydrates and glycoconjugates. Several synthetic analogs have found their way into the clinical use, including the anticoagulant Fondaparinux (Arixtra®) and the antiviral medication Oseltamivir (Tamiflu®). Notwithstanding these advances, the construction of complex carbohydrates and glycoconjugates remains an exceptionally difficult task as there has been no general solution for the stereoselective synthesis of glycosidic linkages.[2–7] To date, the majority of carbohydrate syntheses have been target-oriented, delivering a solution for a single problem. In contrast to these studies, this thesis describes an investigation to the intrinsic reactivity of carbohydrate building blocks as a function of the substitution pattern on the carbohydrate ring. It maps how the combination of the building block reactivities (*i.e.*, the donor and acceptor that are connected in the glycosylation reaction) impacts the mechanism of the glycosylation reaction to shape the outcome of the reaction.

The chemical glycosylation reaction

The central reaction in glycochemistry is the glycosylation reaction, in which two – often expensive – building blocks are united to form more complex (oligo)saccharides. Insufficient knowledge of this reaction thwarts the routine assembly of these materials. In essence, the glycosylation reaction is a substitution reaction between a nucleophile and an electrophile. Figure 1 depicts the general mechanism for the glycosylation reaction, in which the first step consists of the activation of a donor molecule by a promotor system.[4,5,8,9] This activation leads to an array of reactive intermediates, including covalent species, which can undergo S_N2-like substitutions, while cationic intermediates can partake in S_N1-like reactions. The true S_N2- and S_N1-pathways can be found at the extremes of a substitution reaction mechanism continuum that fills the space between these two archetypal reaction mechanisms. Where along the continuum a given glycosylation reaction will take place is heavily influenced by the nature of both reaction partners, the acceptor (*i.e.*, nucleophile) and the donor (*i.e.*, electrophile). The configuration, conformation, and stereoelectronic effects of the ring substituents of both reactants are of all-importance to the reaction mechanism. External factors such as the temperature, concentration and solvent can also change the course of the glycosylation reaction.[2,7–9]

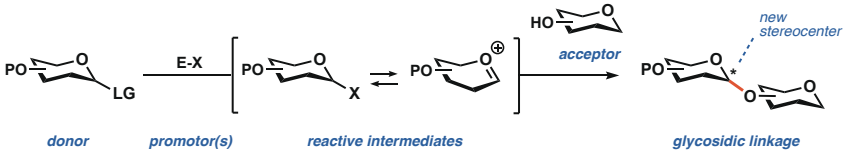

Figure 1. General overview of the glycosylation reaction. Glycosylation reactions are best considered as taking place at a continuum between two formal extremes of the mechanisms, the S_N1- and S_N2-mechanism.

Glycosyl cations: reactivity

Glycosyl cations, also known as oxocarbenium ions, are essential reactive intermediates in glycosylation reactions. These highly reactive intermediates have a short but significant lifetime in aqueous solution, while in less polar organic solvents these species are substantially less stable.[10] The stability of the glycosyl cation is influenced by the substituents present on the carbohydrate ring. Electron-withdrawing substituents (*e.g.* oxygen- or nitrogen-based) have a destabilizing effect on the glycosyl cation. The stability is also affected by the position and orientation of the substituent on the ring. The combined effect of all substituents on the ring determines the stability of the glycosyl cation. The stability of the glycosyl oxocarbenium ions translates to the reactivity of glycosyl donors. The functional groups on glycosyl donor molecules (most commonly hydroxyl and amino groups) are generally protected to reduce unwanted side reactions. It has long been known that the nature of the protecting groups can have a profound effect on the reaction rate and the stereochemical outcome of a glycosylation reaction. In 1982 the group of Paulsen noted that glycosyl halide donors carrying acyl protecting groups were significantly more stable than the corresponding alkylated donors.[11,12] Later, Fraser-Reid and co-workers

conceptualized this reactivity difference in the development of armed-disarmed glycosylation reactions (Figure 2A).[13–15] They showed that *O*-pentenyl glycosides that bear alkyl protecting groups can be selectively activated over *O*-pentenyl glycosides, featuring electron-withdrawing acyl groups. The electron-withdrawing effect of the acyl groups retards the development of positive charge at the anomeric center upon expulsion of the activated anomeric leaving group. The synthesis of trisaccharide **6** shows the applicability of the armed-disarmed concept. In the presence of disarmed pentenyl glycoside **2**, armed donor **1** selectively reacts with the mild activator, iodonium dicollidine perchlorate (IDCP) to furnish the pentenyl disaccharide. Changing the acyl protecting groups in the resulting disaccharide to benzyl ethers 'arms' the disaccharide setting the stage for a second IDCP mediated glycosylation reaction to deliver the trisaccharide.

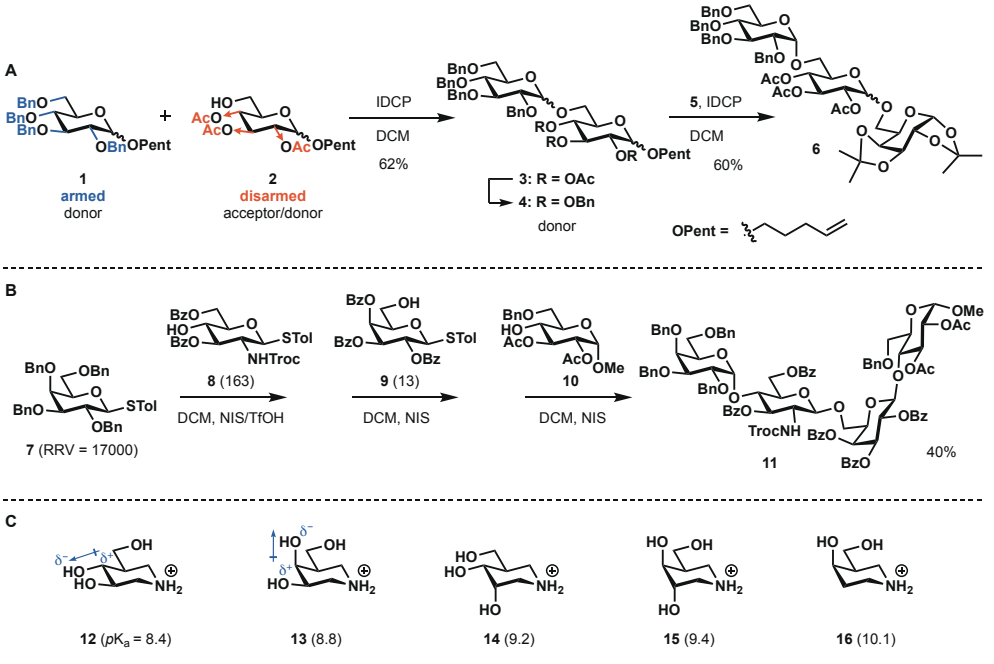

Figure 2. (A) Trisaccharide synthesis of the group Fraser-Reid using the armed-disarmed concept; (B) Tetrasaccharide synthesis of the group of Wong illustrating the continuum of reactivities of the donor molecules; (C) pK_a trends found for substituted piperidines by the group of Bols.

Later, it became apparent that the reactivity of donor glycosides should not be viewed as either armed or disarmed but rather as a continuum of reactivity, and that the nature of the protection groups, the configuration and type of carbohydrate donor all influence the reactivity. Ley and co-workers, followed closely by Wong and co-workers, set out to quantify donor reactivity using a broad range of donor glycosides. Wong and co-workers have compiled large donor reactivity data sets, showing relative donor reactivity to span over eight orders of magnitude. With these data, clear structure-reactivity relationships could be defined for these donors.[16–18] This has enabled the rational design of reactivity-based one-pot glycosylation strategies, an example of which is depicted in Figure 2B.

Galactosyl donor **7**, bearing solely benzyl ethers, has a relative reactivity value (RRV) of 17000, and can be activated selectively over trichloroethoxy carbamate protected glucosamine **8** (RRV = 163) using *N*-iodosuccinimide and triflic acid to provide the galactose-glucosamine disaccharide. Addition of galactose building block **9** (RRV = 13), and additional NIS than leads to the formation of the intermediate trisaccharide which can react with glucose acceptor **10** to deliver tetrasaccharide **11** in 40% yield.

The group of Bols has drawn the parallel between glycosyl donor reactivity and the pK_a-value of iminosugars (Figure 2C).[19,20] They found that the galactose configured iminosugar **13** is 0.4 pK_a units more basic compared to the corresponding gluco-configured piperidine **12**.[19] With a broad panel of different iminosugars they were able to relate the established pK_a-differences to differences in charge-dipole interactions of axially and equatorially oriented hydroxyl groups. They concluded that equatorially oriented hydroxyls are more electron withdrawing than their axially oriented counterparts.[21,22]

Glycosyl cations: stability, selectivity and shape

To investigate the influence of glycosyl substituents on the stereoselectivity of glycosylation reactions proceeding at the S_N1-side of the reaction continuum, the group of Woerpel has systematically studied *C*-glycosylation reactions of a set of furanosyl and pyranosyl donors.[23–32] Their studies in the furanose series are summarized in Figure 3A. They found that the alkoxy groups at the C2- and C3-position have a strong influence on the stereochemical outcome of the reaction, providing the *cis*-products, while the alkoxy group at the C5-position appears to have less effect on the stereoselective outcome.[23,25]

To account for these stereodirecting substituent effects, they devised a model (Figure 3B) that takes into account the equilibrium between two possible envelope oxocarbenium ion conformers (^3E and E_3).[25] In the ^3E and E_3 the flat C2-C1=O4$^+$-C4 system allows for stabilization of the electron depleted anomeric carbon by the C4-oxygen. Nucleophilic addition to these furanosyl cation conformers occurs from the 'inside' of the envelopes, which avoid unfavorable eclipsing interactions between the C1-*H* and the *pseudo*-equatorial substituent at the C2-position. Additionally, it also avoids unfavorable interaction between the incoming nucleophile and the axial C2-substituent.

The spatial orientation of the alkoxy groups influences the shape and stability of furanosyl cations. A *pseudo*-equatorial position of the C2-substituent enables hyperconjugative stabilization of the furanosyl cation by the *pseudo*-axially oriented C2-H2 bond (Figure 3C). Stabilization of the furanosyl cation featuring a C3-alkoxy group is achieved by placing the electronegative substituent in an axial fashion, thereby providing a stabilizing electrostatic interaction (Figure 3C). With these spatial substituent preferences, the stereochemical outcome of the *C*-glycosylation reactions in Figure 3A can be explained. Activation of the C2-benzyloxy furanosyl acetate **17** provides a furanosyl cation intermediate that preferentially adopts a ^3E conformation. Nucleophilic addition on this conformer takes place in an inside fashion that leads to the 1,2-*cis* product. By a similar mechanism, inside nucleophilic addition on the ^3E conformer of the C3-benzyloxy

furanosyl cation, derived from furanosyl acetate **18**, accounts for the stereochemical outcome of the *C*-glycosylation. The oxocarbenium ion derived from C4-benzyloxy protected **19** has no clear conformational preference, which results in a stereochemical mixture of products.

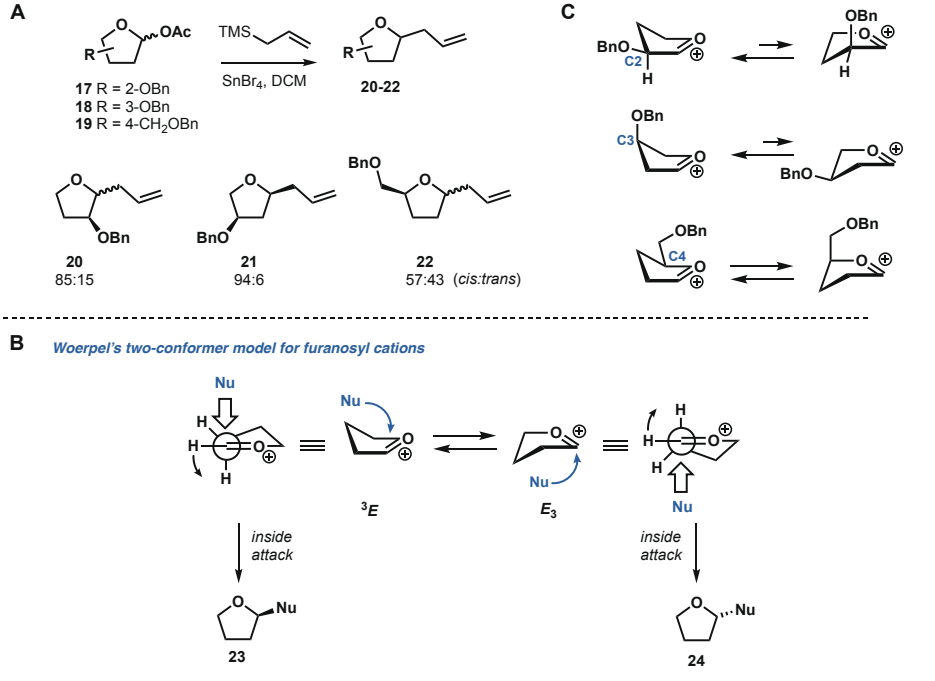

Figure 3. Stereochemical preference of furanosyl cations. (A) Stereochemical outcome of *C*-glycosylation of a set of mono-substituted furanosyl acetates, in which the *cis*:*trans* ratio is expressed as the relationship between the substituent and the coupled nucleophile; (B) Two-conformer model proposed by the group of Woerpel; (C) Conformational preference of mono-substituted furanosyl cations.

To analyze the combined effect of multiple substituents on the furanosyl cation, van Rijssel *et al.*[33–36] adopted a computational method, initially developed by Rhoad and co-workers.[37] This computational method calculates the energy of all furanosyl oxocarbenium ion conformers, which can be plotted on the pseudorotational circle introduced by Altona and Sundaralingam (Figure 4C). The conformational energy landscapes (CEL) of four fully decorated diastereoisomeric furanosyl oxocarbenium ions were generated, revealing the lowest energy conformers for the ribo-, arabino-, xylo- and lyxo-configured furanosyl oxocarbenium ions (Figure 4B). Based on the computed CEL maps, the stereoselectivity of S_N1-type glycosylation reactions of the four diastereoisomeric furanosyl acetates **25-28** could be explained (Figure 4A). All four furanosides reacted in a 1,2-*cis* selective fashion when activated by TMSOTf in the presence of triethylsilane-*d* (TES-*d*), and only xylofuranosyl acetate **27** provided some of the 1,2-*trans* product. The erosion of stereochemistry for the xylofuranosyl cation could be related to the relative stability of the ^3E furanosyl cation intermediate (ΔE = 1.0 kcal mol^{-1}).

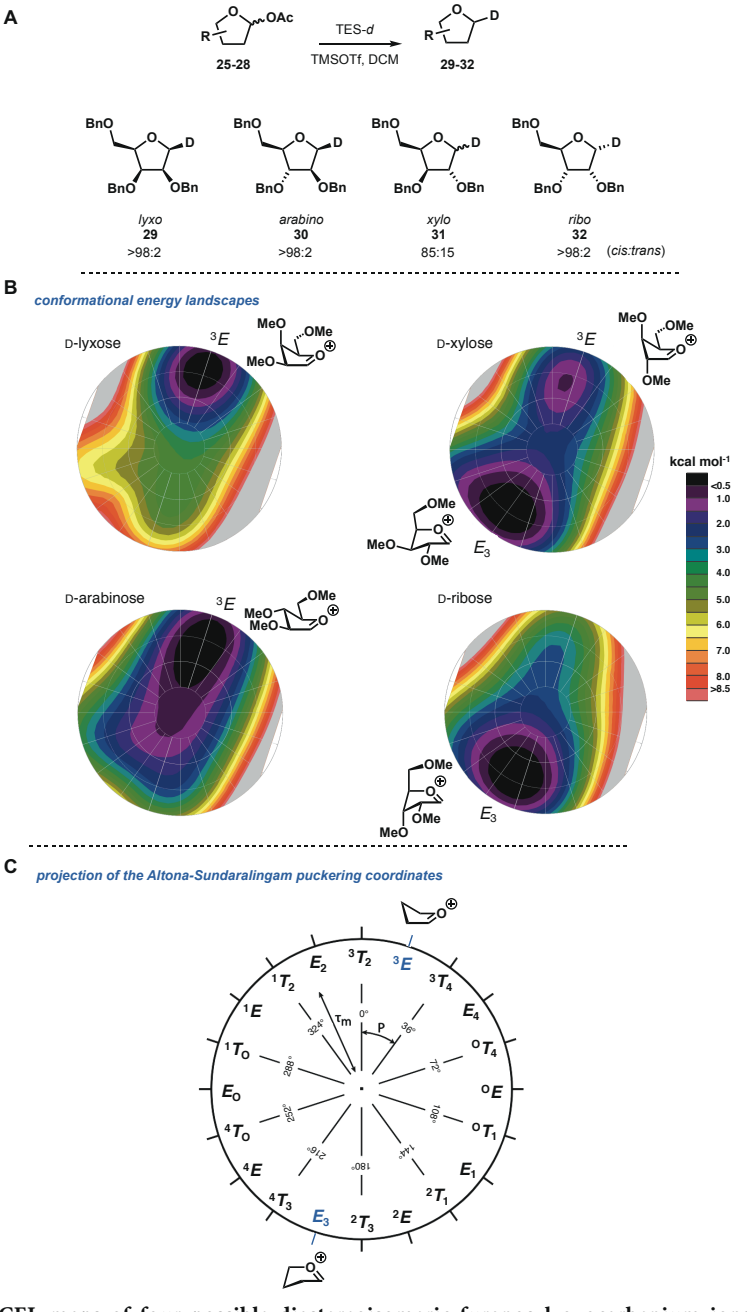

Figure 4. CEL maps of four possible diastereoisomeric furanosyl oxocarbenium ions and the diastereoselective reductions of furanosyl acetates. (A) Experimentally found stereoselectivities of model glycosylation reactions with TES-*d* as nucleophile; (B) CEL maps in which the local minima are shown. All energies are as computed at PCM(CH_2Cl_2)-B3LYP/6-311G(d,p) and expressed as the solution-phase electronic energy; (C) The pseudorotational circle describing the complete conformational space a five-membered ring can occupy. The pseudorotational phase angle (P) in combination with the puckering amplitude (τ_m) defines the ring conformation.

The above-described substituent effects can also be found in related, charged or strongly polarized six-membered ring systems, as illustrated in Figure 5.[38–40] Figure 5A depicts that an electronegative groups at C4 of a cyclohexanone takes up an axial position to maximize electrostatic stabilization of the electron poor ketone carbon, lowering the total energy of the system.[29,30,41,42] This is also the case for the glycosidase inhibitor depicted in Figure 5B, which adopts an "all-axial" conformer to maximize the electrostatic stabilization of the sulfonium cation.[43] Even though this introduces a significant amount of steric interactions, this is not sufficient to override the electrostatic stabilization. Substituents at a position next to an electron depleted carbon (*i.e.*, C2-position) will preferentially adopt an orientation to allow for optimal hyperconjugative stabilization (Figure 5C).[32,44] In cyclohexanone **37**-**38**, the C-F bond is a much weaker σ-donor than the C-H bond, and therefore the C-F is placed in a *pseudo*-equatorial position. In contrast, the C-I bond is a significantly stronger σ-donor than the C-H bond, and therefore C-2-iodo cyclohexanone **40**, having C-I bond in a *pseudo*-axial orientation, is more stable than conformer **39**.

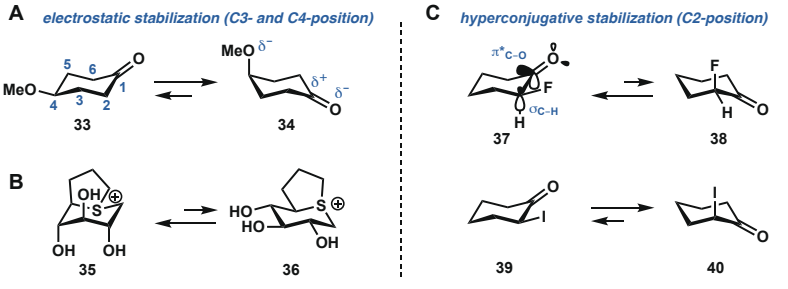

Figure 5. Electrostatic and hyperconjugative stabilization can have a dramatic effect on the conformational preferences of charged or strongly polarized six-membered rings. (A) Electronegative groups on the C3- and C4-position of cyclohexanone favor a *pseudo*-axial position; (B) Glycosidase inhibitor adopts an all-axial conformation as a result of stabilizing electrostatic interactions; (C) Hyperconjugation capacity gives rise to a clear conformational trend when comparing different halides present on the 2-position of cyclohexanones.

In parallel to the stereoelectronic substituent effects found in the 5-membered ring series, the group of Woerpel and others investigated 6-membered ring systems.[26–28,45,46] In line with the effects observed in the 5-membered ring series, the stability of these cations benefits from a *pseudo*-equatorial orientation of the alkoxy group on the C2-position (allowing for hyperconjugative stabilization by the $\sigma_{C2\text{-}H2}$ bond), and an axial orientation of the alkoxy groups on the C3- and C4-positions.[28] The alkoxymethylene group on the C5-position has a preference for an equatorial position for steric reasons.[26] The group of Woerpel reasoned that pyranosyl cations preferentially adopt a $^{3}H_{4}$ or $^{4}H_{3}$ half-chair structure to accommodate the flat C2-C1=O5^{+}-C5 oxocarbenium ion moiety (Figure 6B).[28] The addition reactions to these half-chair intermediates by incoming nucleophiles preferentially follow a trajectory that leads to a chair-like transition state. Thus, the addition to a $^{3}H_{4}$ half-chair occurs from the top-face, whereas addition to the opposite $^{4}H_{3}$ half-chair

leads to the bottom-face product. With the above described spatial substituent preferences and mode of nucleophilic addition, the stereochemical outcome in the *C*-glycosylation reactions shown in Figure 6A can be accounted for. The C2-OBn is *cis*-directing, where the C3-OBn forms in excellent selectivity the *cis*-product, and the C4-OBn forms exclusively the *trans*-product.

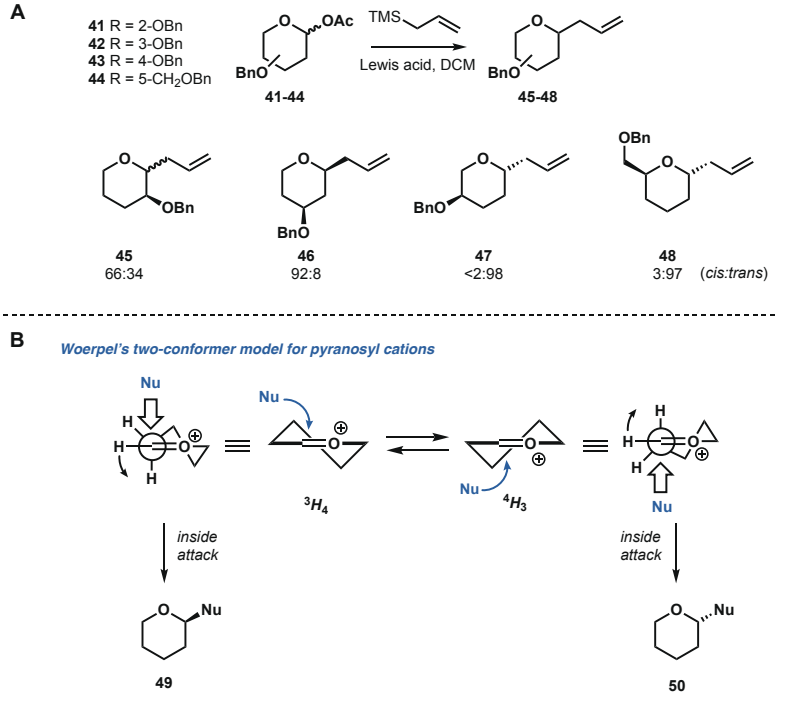

Figure 6. Stereochemical preference of pyranosyl cations. (A) Stereochemical outcome of *C*-glycosylations of a set of mono-substituted pyranosyl acetates, in which the *cis*:*trans* ratio is expressed as the relationship between the substituent and the coupled nucleophile; (B) Two-conformer model proposed by the group of Woerpel.

To accurately gauge the combined substituent effects on the conformational behavior, reactivity and stability of pyranosyl oxocarbenium ions, several computational studies have been undertaken (see Figure 7B).[47–53] The conformational space of pyranosyl oxocarbenium ion can be visualized by the use of the Cremer–Pople sphere (Figure 7C), and all possible conformations can be plotted on this "sphere". Whitfield and co-workers have investigated the conformational preference of tetra-*O*-methyl-gluco- and tetra-*O*-methyl-mannopyranosyl oxocarbenium ions (**59** and **60**) as well as their 4,6-*O*-benzylidene analogs (**61** and **62**). They studied the conformational behavior of the oxocarbenium ions, formed upon dissociation of the triflate leaving group.[50] In these studies a lithium cation was used to stabilize the anionic leaving group upon departure. These computations revealed that dissociation of the tetra-*O*-methyl gluco- and tetra-*O*-methyl-mannopyranosyl α-triflates initially provides the $^4H_3$ oxocarbenium ion for both pyranosides (Figure 7B).

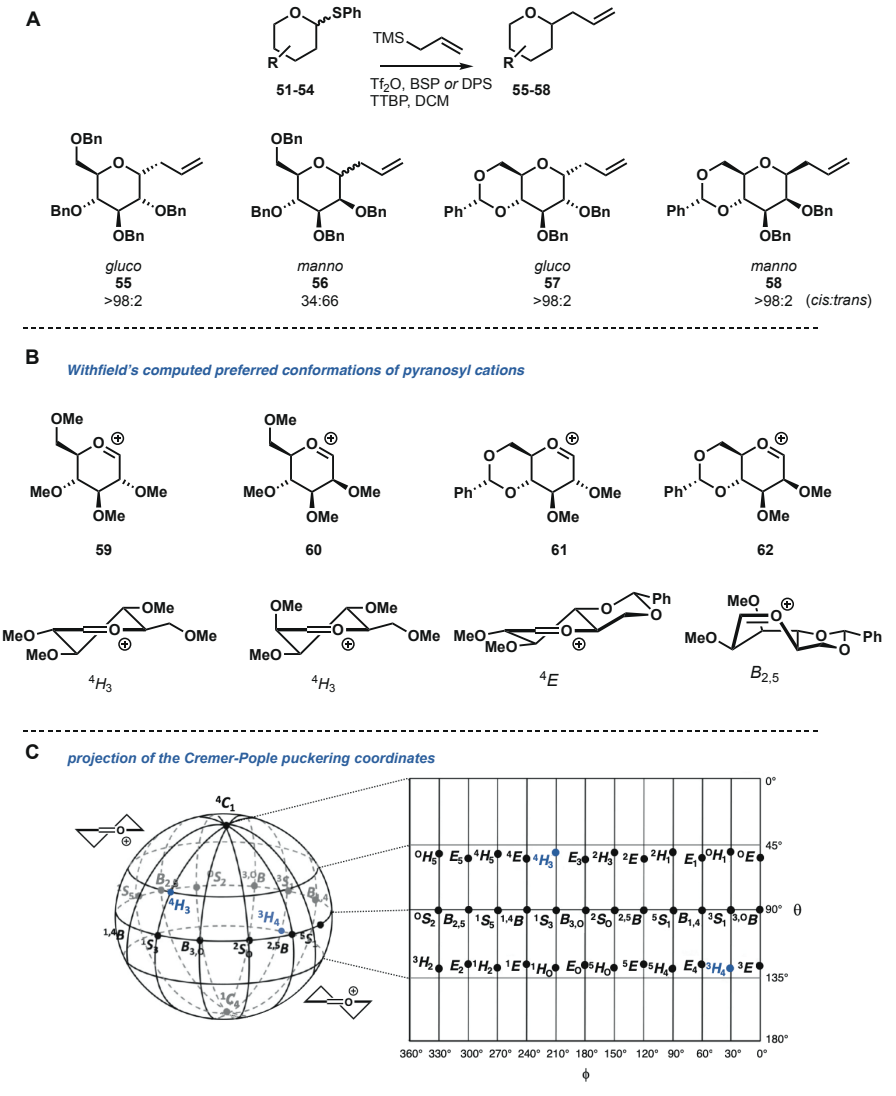

Figure 7. Computational data of selected pyranosyl oxocarbenium ions and the diastereoselective *C*-glycosylations of pyranosyl donors. (A) Experimentally found stereoselectivities for model glycosylation reactions with allyltrimethylsilane as nucleophile; (B) Selection of oxocarbenium ions and their computed solution-phase energies by density functional theory (DFT); (C) Cremer–Pople sphere which is a spherical representation describing all possible conformations a six-membered ring can adopt.

Dissociation of the triflate from the β-stereoisomers requires a conformational change, where the glucose and mannose pyranosyl rings distort to a $^{1}S_{3}$-like structure.[50] In this geometry, the anomeric leaving group can be dissociated by assistance of the ring oxygen leading to a ^{4}E (for the glucose case) or $^{4}H_{3}$ half chair (for the mannose case).

Similar itineraries have been established to be operational in glycosyl hydrolases. The group of Rovira has found for retaining glucosyl hydrolases, that hydrolysis of β-glucosides proceeds via a trajectory in which the substrate is first placed in a $^{1}S_{3}$ conformation which allows for dissociation of the aglycon.[54,55] After passing through a $^{4}H_{3}$-like transition state, the $^{4}C_{1}$ product (the covalent enzyme-glucose adduct) is formed. This catalytic itinerary was established using a combination of X-ray crystallography, free energy landscape mapping, and QM/MM simulations.

The Whitfield group showed that the 4,6-*O*-benzylidene glucose oxocarbenium ion **61** preferentially take up a ^{4}E conformer, while the corresponding benzylidene-mannose structure **62**, takes up a $B_{2,5}$ conformation.[50] In the latter structure, both the electrostatic interaction by the C3-OMe and hyperconjugative stabilization of the $\sigma_{C2\text{-}H2}$ bond contributes to the stability of the mannosyl cation. Based on the computed preferred conformations, the stereoselectivity of the *C*-glycosylation reactions of a set of glucosyl- and mannosyl donors (**51**-**54**) could be explained (Figure 7A).[45,56] The glucosyl derivatives (**51** and **53**) both form exclusively the 1,2-*cis* product, which could be explained by a bottom-face addition of the nucleophile to the $^{4}H_{3}$-like structure. For mannosyl donor **52** a 1,2-*trans* preference was found, which could be explained by a bottom-face addition on the $^{4}H_{3}$, while for mannosyl donor **54** a top-face addition on the $B_{2,5}$ structure results in exclusive formation of the 1,2-*cis* product.

Glycosyl cations: experimental observation

To date, many anomeric triflates, the reactive intermediates on the S_N2-side of the glycosylation reaction mechanism manifold, have been spectroscopically characterized by variable temperature NMR experiments. In contrast, the intrinsic high reactivity of glycosyl cations hampers their straightforward detection. The group of Woerpel have used pyranosyl dioxocarbenium ions (Figure 8A) as a stabilized analogue of the corresponding oxocarbenium ion.[30] They computed the expected conformational preference and correlated this with the experimentally determined $^{3}J_{H\text{-}H}$ NMR coupling constants. This supported the proposed axial preference of alkoxy-substituents at the C3- and the C4-position.

The group of Blériot reported the generation and spectroscopic investigation of glycosyl cations by the use of a superacid medium (*i.e.*, HF/SbF_5).[57,58] The cations, generated in this non-nucleophilic solvent proved to be stable for several hours at −40 °C in the superacid medium, which allowed the full characterization of these species. Figure 8B shows the conversion of 2-deoxy-glucosyl donor **65** into the glycosyl cation adopting a ^{4}E conformation. The conformation of the cation was deduced from the $^{3}J_{H\text{-}H}$ coupling constants and supported by DFT computations and simulated spectra. Trapping of the glycosyl cation **66** by cyclohexane-d_{12} resulted in the selective formation of an α-deuterated 2-deoxy-glucoside. The formation of this product can be accounted for using the found ^{4}E conformer, which forms the α-product through a chair-like bottom-face addition reaction.

Obviously, the solvent system used in these NMR experiments deviates significantly from the conditions used in normal glycosylation reactions, and therefore, care should be taken in the translation of the results obtained in the superacid medium. Nonetheless, this study has provided fundamental information on the conformational preference of glycosyl cations.

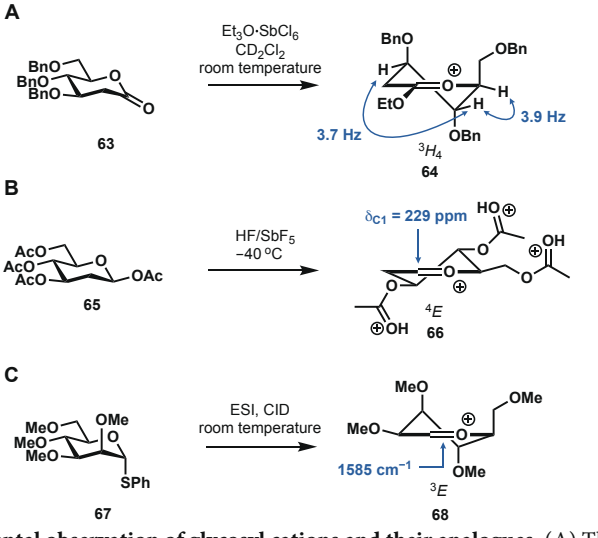

Figure 8. Experimental observation of glycosyl cations and their analogues. (A) The formation of a dioxocarbenium ion by treating a lacton with Meerwein's salt; (B) Generation of a 2-deoxy-glucosyl cation in HF/SbF_5; (C) The formation of a mannosyl cation by the use of collision induced dissociation tandem mass spectrometry.

Recently, also the groups of Boltje and Pagel reported on the formation and analysis of glycosyl oxocarbenium ions (Figure 8C).[59–61] They used collision induced dissociation tandem mass spectrometry, which generates glycosyl cations in the gas-phase followed by infrared ion spectroscopy. The experimentally observed IR spectra were compared with DFT computed spectra, enabling the detailed structural elucidation of the glycosyl cations. For mannose donor **67**, mannosyl cation **68** with a ^3E conformation was established. Also, with this method care should be taken in the translation of the results obtained in the gas-phase at room temperature to experimental glycosylation reactions taking place in an organic reaction medium, often at low temperatures.

Glycosyl cations: product-forming reactive intermediates

The group of Crich used kinetic isotope effect (KIE) experiments to generate proof for glycosyl cations as product-forming intermediates.[62,63] Using natural abundance ^{13}C primary KIEs, in combination with DFT calculations, they analyzed the amount of carbocation character that builds up in the transition state of the reactions shown in Figure 9A. The systems that were studied included glycosylations of 2-propanol with either a benzylidene protected mannosyl **69** or glycosyl donor **76**.[62] From the experimental and

computed KIE values, it was deduced that the β-mannosyl product was formed through an associative pathway, in which the S_N2-like transition state passes through a $B_{2,5}$ conformation. In contrast, the α-mannosyl product originated from a more dissociative mechanism, involving a mannosyl cation. The DFT calculations suggested a $^4E/^4H_3$-like conformation for the intermediate mannosyl cation.

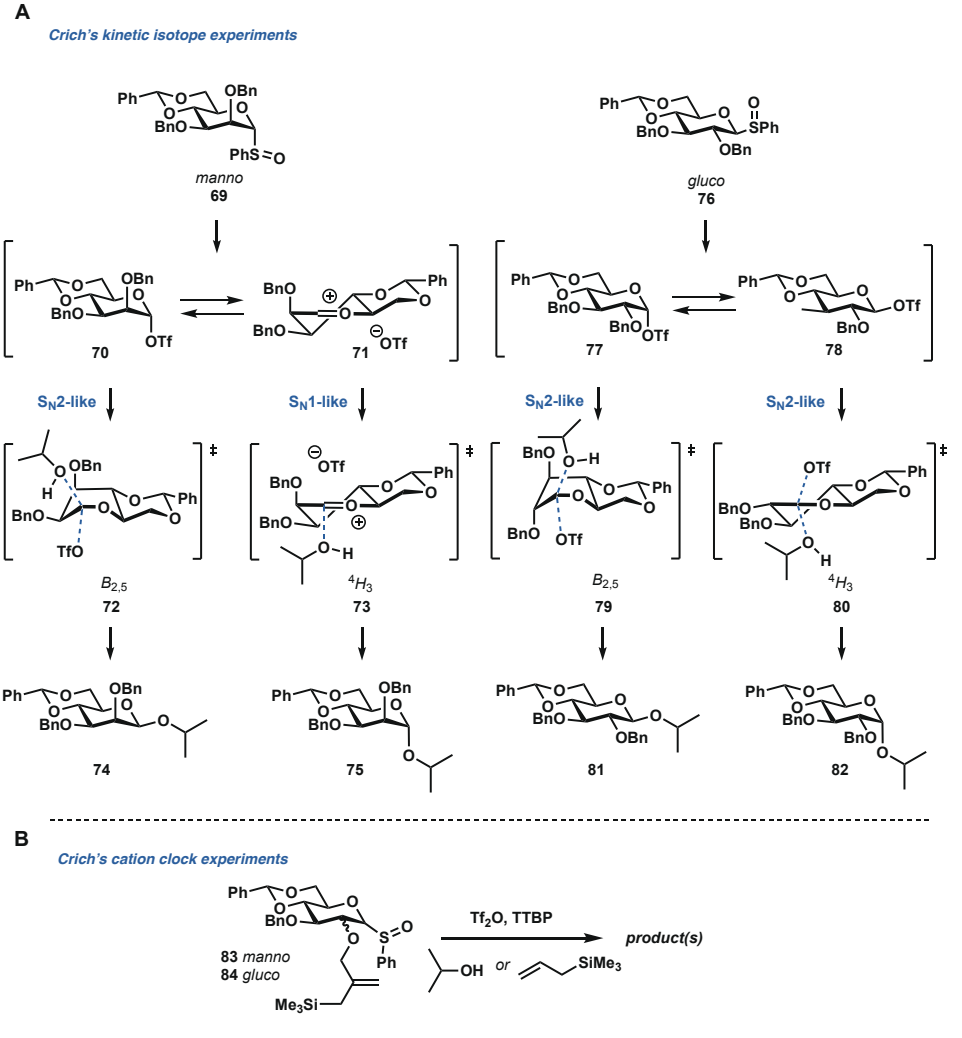

Figure 9. Product forming pathways for benzylidene mannosylations and glucosylations. (A) Reaction mechanistic results based on natural abundance ^{13}C primary kinetic isotope effects; (B) Reaction mechanistic results based on the cation clock method.

For the benzylidene glucose system, it was found that both the α- and β-products were formed through an associative S_N2-like mechanism.[62]

In parallel, the group of Crich developed cation clock methodology, which is shown in Figure 9B.[64,65] In this method external nucleophiles (*i.e.*, 2-propanol or allyltrimethylsilane) are used to compete with an intramolecular nucleophilic cyclization reaction. Using mannosyl and glucosyl donors **83** and **84**, they showed that the *O*-glycosylations are more concentration dependent than the *C*-glycosylation reactions.[64,65] Using this method, they found that the formation of the *O*-mannosyl α- and β-products results from different mechanistic pathways. For the α-product an S_N1-like pathway was found, while the β-products were formed through an S_N2-like pathway. When allyltrimethylsilane was employed as a nucleophile, only the β-*C*-allyl mannosyl and α-*C*-allyl glucosyl products were obtained in a reaction that was relatively independent of the concentration of the nucleophile, indicating the presence of significant S_N1-like character in these reactions.

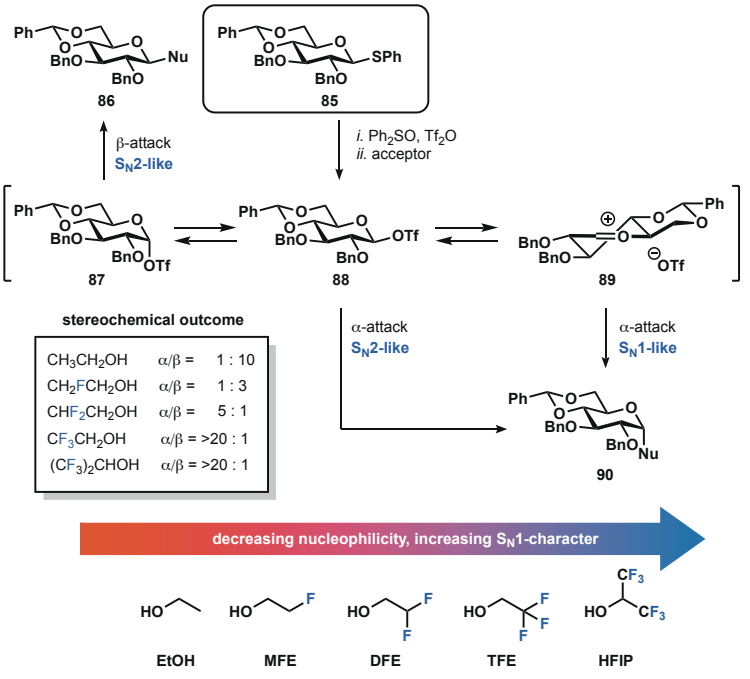

Figure 10. Found mechanistic continuum operational during the glycosylation of donor **73** with a set of model nucleophiles.

Van der Vorm *et al.* also provided evidence for the involvement of glycosyl cation-like species in *O*-glycosylation reactions (Figure 10).[45,46,66] They performed an array of glycosylation reactions with a set of model (fluorinated) alcohol nucleophiles (*i.e.*, EtOH, MFE, DFE, TFE and HFIP) of gradually decreasing nucleophilicity. This revealed that the stereoselectivity in glycosylations of benzylidene protected glucose donors are very

susceptible to acceptor nucleophilicity. Reactions of this donor proceeded with stereoselectivity, ranging from complete β-selectivity to the exclusively formation of the α-product (Figure 9). They related this reactivity-selectivity relationship to changes from an S_N2-type substitution of the covalent intermediate (*e.g.*, α-glycosyl triflate) for the most nucleophilic alcohols to reactions involving more oxocarbenium character for the poorest nucleophiles (*i.e.*, TFE and HFIP).

Summary and thesis outline

Glycosyl cations are essential reactive intermediates in glycosylation reactions. Although significant progress has been made in the field, studying these highly reactive intermediates remains a major challenge and lies at the forefront of current efforts to advance glycosylation knowledge. The research described in this thesis aims to gain more fundamental insight into the mechanisms of chemical glycosylation reactions and their reactive intermediates. Chapter 2 introduces a novel computational approach to study the shape of glycosyl cations as a function of their substitution pattern. More than 30 different glycosyl donors with varying substituents are evaluated. To connect the computational efforts to experimental results, all studied cations are subjected to a set of model S_N1-glycosylations. Selected glycosyl cations are also generated under superacid conditions, which allowed the direct observation of these highly reactive intermediates. Chapter 3 expands on Chapter 2 focusing on the transition state of the addition reaction between the glycosyl cation and the acceptor. Using typical S_N1-nucleophiles, it is found that the course of the addition reaction to some cations is very susceptible to the nature of the used nucleophile, with an opposite stereochemical outcome found for different nucleophiles. Using computational methods, Curtin-Hammett kinetic scenarios are dissected to account for the observed results. The subject of Chapter 4 covers the possible formation of dioxolenium ions through remote acyl groups present on donor molecules, which can result in long-range participation and steering of the stereochemical outcome of glycosylation reactions. This chapter reports an integrated approach, using infrared ion spectroscopy, DFT calculations and a systematic series of glycosylation reactions to probe these ions and their relevance for the glycosylation reaction. The research described in Chapter 5 implements the fundamental insight gained in the previous chapters in the assembly of a biologically relevant complex mycobacterial glycolipid, built up from (amongst others) rare and complex monosaccharides, featuring tertiary stereocenters. By using variable-temperature NMR, DFT computations, and model glycosylations, the rational design of caryophyllose acceptor and donor molecules with the desired properties was possible. This enabled the assemble of a fragment of the LOS-IV lipooligosaccharide and related shorter fragments, present in *Mycobacterium marinum*, a closely related bacterium to *Mycobacterium tuberculosis*. Chapter 6 provides a summary of the results described in this thesis, as well as an outlook for further investigations to unravel the details of the glycosylation mechanism.

References

(1) Seeberger, P. H.; Werz, D. B. Synthesis and Medical Applications of Oligosaccharides. *Nature* **2007**, *446* (7139), 1046–1051.

(2) A. V. Demchenko. *Handbook of Chemical Glycosylation: Advances in Stereoselectivity and Therapeutic Relevance*; Wiley, **2008**.

(3) Zhu, X.; Schmidt, R. R. New Principles for Glycoside-Bond Formation. *Angew. Chem. Int. Ed.* **2009**, *48* (11), 1900–1934.

(4) Bohé, L.; Crich, D. A Propos of Glycosyl Cations and the Mechanism of Chemical Glycosylation; the Current State of the Art. *Carbohydr. Res.* **2015**, *403*, 48–59.

(5) Bohé, L.; Crich, D. A Propos of Glycosyl Cations and the Mechanism of Chemical Glycosylation. *Comptes Rendus Chimie* **2011**, *14* (1), 3–16.

(6) Boltje, T. J.; Buskas, T.; Boons, G.-J. Opportunities and Challenges in Synthetic Oligosaccharide and Glycoconjugate Research. *Nat. Chem.* **2009**, *1* (8), 611–622.

(7) Nigudkar, S. S.; Demchenko, A. V. Stereocontrolled 1,2-*Cis* Glycosylation as the Driving Force of Progress in Synthetic Carbohydrate Chemistry. *Chem. Sci.* **2015**, *6* (5), 2687–2704.

(8) Adero, P. O.; Amarasekara, H.; Wen, P.; Bohé, L.; Crich, D. The Experimental Evidence in Support of Glycosylation Mechanisms at the S_N1–S_N2 Interface. *Chem. Rev.* **2018**, *118* (17), 8242–8284.

(9) Mydock, L. K.; Demchenko, A. V. Mechanism of Chemical *O*-Glycosylation: From Early Studies to Recent Discoveries. *Org. Biomol. Chem.* **2010**, *8* (3), 497–510.

(10) Amyes, T. L.; Jencks, W. P. Lifetimes of Oxocarbenium Ions in Aqueous Solution from Common Ion Inhibition of the Solvolysis of α-Azido Ethers by Added Azide Ion. *J. Am. Chem. Soc.* **1989**, *111* (20), 7888–7900.

(11) Paulsen, H. Advances in Selective Chemical Syntheses of Complex Oligosaccharides. *Angew. Chem. Int. Ed.* **1982**, *21* (3), 155–173.

(12) Paulsen, H. Fortschritte bei der selektiven chemischen Synthese komplexer Oligosaccharide. *Angew. Chem.* **1982**, *94* (3), 184–201.

(13) Fraser-Reid, B.; Udodong, U. E.; Wu, Z.; Ottosson, H.; Merritt, J. R.; Rao, C. S.; Roberts, C.; Madsen, R. *N*-Pentenyl Glycosides in Organic Chemistry: A Contemporary Example of Serendipity. *Synlett* **1992**, *1992* (12), 927–942.

(14) Mootoo, D. R.; Konradsson, Peter.; Udodong, Uko.; Fraser-Reid, Bert. Armed and Disarmed *N*-Pentenyl Glycosides in Saccharide Couplings Leading to Oligosaccharides. *J. Am. Chem. Soc.* **1988**, *110* (16), 5583–5584.

(15) Fraser-Reid, B.; Wu, Z.; Udodong, U. E.; Ottosson, H. Armed/Disarmed Effects in Glycosyl Donors: Rationalization and Sidetracking. *J. Org. Chem.* **1990**, *55* (25), 6068–6070.

(16) Zhang, Z.; Ollmann, I. R.; Ye, X.-S.; Wischnat, R.; Baasov, T.; Wong, C.-H. Programmable One-Pot Oligosaccharide Synthesis. *J. Am. Chem. Soc.* **1999**, *121* (4), 734–753.

(17) Mong, K.-K. T.; Wong, C.-H. Reactivity-Based One-Pot Synthesis of a Lewis Y Carbohydrate Hapten: A Colon–Rectal Cancer Antigen Determinant. *Angew. Chem.* **2002**, *114* (21), 4261–4264.

(18) Hsu, C.-H.; Hung, S.-C.; Wu, C.-Y.; Wong, C.-H. Toward Automated Oligosaccharide Synthesis. *Angew. Chem. Int. Ed.* **2011**, *50* (50), 11872–11923.

(19) Jensen, H. H.; Lyngbye, L.; Jensen, A.; Bols, M. Stereoelectronic Substituent Effects in Polyhydroxylated Piperidines and Hexahydropyridazines. *Chem. Eur. J.* **2002**, *8* (5), 1218–1226.

(20) Jensen, H. H.; Bols, M. Synthesis of 1-Azagalactofagomine, a Potent Galactosidase Inhibitor. *J. Chem. Soc., Perkin Trans. 1* **2001**, No. 8, 905–909.

(21) Pedersen, C. M.; Nordstrøm, L. U.; Bols, M. "Super Armed" Glycosyl Donors: Conformational Arming of Thioglycosides by Silylation. *J. Am. Chem. Soc.* **2007**, *129* (29), 9222–9235.

(22) Pedersen, C. M.; Marinescu, L. G.; Bols, M. Conformationally Armed Glycosyl Donors: Reactivity Quantification, New Donors and One Pot Reactions. *Chem. Commun.* **2008**, No. 21, 2465–2467.

(23) Larsen, C. H.; Ridgway, B. H.; Shaw, J. T.; Woerpel, K. A. A Stereoelectronic Model To Explain the Highly Stereoselective Reactions of Nucleophiles with Five-Membered-Ring Oxocarbenium Ions. *J. Am. Chem. Soc.* **1999**, *121* (51), 12208–12209.

(24) Shaw, J. T.; Woerpel, K. A. Divergent Diastereoselectivity in the Addition of Nucleophiles to Tetrahydrofuran-Derived Oxonium Ions. *Tetrahedron* **1999**, *55* (29), 8747–8756.

(25) Larsen, C. H.; Ridgway, B. H.; Shaw, J. T.; Smith, D. M.; Woerpel, K. A. Stereoselective *C*-Glycosylation Reactions of Ribose Derivatives: Electronic Effects of Five-Membered Ring Oxocarbenium Ions. *J. Am. Chem. Soc.* **2005**, *127* (31), 10879–10884.

(26) Lucero, C. G.; Woerpel, K. A. Stereoselective *C*-Glycosylation Reactions of Pyranoses: The Conformational Preference and Reactions of the Mannosyl Cation. *J. Org. Chem.* **2006**, *71* (7), 2641–2647.

(27) Romero, J. A. C.; Tabacco, S. A.; Woerpel, K. A. Stereochemical Reversal of Nucleophilic Substitution Reactions Depending upon Substituent: Reactions of Heteroatom-Substituted Six-Membered-Ring Oxocarbenium Ions through Pseudoaxial Conformers. *J. Am. Chem. Soc.* **2000**, *122* (1), 168–169.

(28) Ayala, L.; Lucero, C. G.; Romero, J. A. C.; Tabacco, S. A.; Woerpel, K. A. Stereochemistry of Nucleophilic Substitution Reactions Depending upon Substituent: Evidence for Electrostatic Stabilization of Pseudoaxial Conformers of Oxocarbenium Ions by Heteroatom Substituents. *J. Am. Chem. Soc.* **2003**, *125* (50), 15521–15528.

(29) Chamberland, S.; Ziller, J. W.; Woerpel, K. A. Structural Evidence That Alkoxy Substituents Adopt Electronically Preferred Pseudoaxial Orientations in Six-Membered Ring Dioxocarbenium Ions. *J. Am. Chem. Soc.* **2005**, *127* (15), 5322–5323.

(30) Yang, M. T.; Woerpel, K. A. The Effect of Electrostatic Interactions on Conformational Equilibria of Multiply Substituted Tetrahydropyran Oxocarbenium Ions. *J. Org. Chem.* **2009**, *74* (2), 545–553.

(31) Beaver, M. G.; Woerpel, K. A. Erosion of Stereochemical Control with Increasing Nucleophilicity: *O*-Glycosylation at the Diffusion Limit. *J. Org. Chem.* **2010**, *75* (4), 1107–1118.

(32) Billings, S. B.; Woerpel, K. A. Nucleophilic Substitution Reactions of Sulfur-Substituted Cyclohexanone Acetals: An Analysis of the Factors Controlling Stereoselectivity. *J. Org. Chem.* **2006**, *71* (14), 5171–5178.

(33) van Rijssel, E. R.; van Delft, P.; Lodder, G.; Overkleeft, H. S.; van der Marel, G. A.; Filippov, D. V.; Codée, J. D. C. Furanosyl Oxocarbenium Ion Stability and Stereoselectivity. *Angew. Chem. Int. Ed.* **2014**, *53* (39), 10381–10385.

(34) van Rijssel, E. R.; van Delft, P.; van Marle, D. V.; Bijvoets, S. M.; Lodder, G.; Overkleeft, H. S.; van der Marel, G. A.; Filippov, D. V.; Codée, J. D. C. Stereoselectivity in the Lewis Acid Mediated Reduction of Ketofuranoses. *J. Org. Chem.* **2015**, *80* (9), 4553–4565.

(35) Madern, J. M.; Hansen, T.; van Rijssel, E. R.; Kistemaker, H. A. V.; van der Vorm, S.; Overkleeft, H. S.; van der Marel, G. A.; Filippov, D. V.; Codée, J. D. C. Synthesis, Reactivity, and Stereoselectivity of 4-Thiofuranosides. *J. Org. Chem.* **2019**, *84* (3), 1218–1227.

(36) van der Vorm, S.; Hansen, T.; van Rijssel, E. R.; Dekkers, R.; Madern, J. M.; Overkleeft, H. S.; Filippov, D. V.; van der Marel, G. A.; Codée, J. D. C. Furanosyl Oxocarbenium Ion Conformational Energy Landscape Maps as a Tool to Study the Glycosylation Stereoselectivity of 2-Azidofuranoses, 2-Fluorofuranoses and Methyl Furanosyl Uronates. *Chem. Eur. J.* **2019**, *25* (29), 7149–7157.

(37) Rhoad, J. S.; Cagg, B. A.; Carver, P. W. Scanning the Potential Energy Surface of Furanosyl Oxocarbenium Ions: Models for Reactive Intermediates in Glycosylation Reactions. *J. Phys. Chem. A* **2010**, *114* (15), 5180–5186.

(38) Smith, D. M.; Woerpel, K. A. Electrostatic Interactions in Cations and Their Importance in Biology and Chemistry. *Org. Biomol. Chem.* **2006**, *4* (7), 1195–1201.

(39) Dibble, D. J.; Ziller, J. W.; Woerpel, K. A. Spectroscopic and X-Ray Crystallographic Evidence for Electrostatic Effects in 4-Substituted Cyclohexanone-Derived Hydrazones, Imines, and Corresponding Salts. *J. Org. Chem.* **2011**, *76* (19), 7706– 7719.

(40) Baghdasarian, G.; Woerpel, K. A. Electrostatic Effects on the Reactions of Cyclohexanone Oxocarbenium Ions. *J. Org. Chem.* **2006**, *71* (18), 6851–6858.

(41) Stolow, R. D.; Giants, T. W. Predominance of the Axial Conformation of 4-Methoxycyclohexanone. *J. Chem. Soc. D* **1971**, No. 11, 528–529.

(42) Baldry, K. W.; Gordon, M. H.; Hafter, R.; Robinson, M. J. T. Conformational Effects in Compounds with 6-Membered Rings—XI : Study of a Conformational Equilibrium in the Gas Phase and in Solvents Ranging from Non-Polar to Water: 4-Methoxycyclohexanone. *Tetrahedron* **1976**, *32* (21), 2589–2594.

(43) Szczepina, M. G.; Johnston, B. D.; Yuan, Y.; Svensson, B.; Pinto, B. M. Synthesis of Alkylated Deoxynojirimycin and 1,5-Dideoxy-1,5-Iminoxylitol Analogues: Polar Side-Chain Modification, Sulfonium and Selenonium Heteroatom Variants, Conformational Analysis, and Evaluation as Glycosidase Inhibitors. *J. Am. Chem. Soc.* **2004**, *126* (39), 12458–12469.

(44) Basso, E. A.; Kaiser, C.; Rittner, R.; Lambert, J. B. Axial/Equatorial Proportions for 2-Substituted Cyclohexanones. *J. Org. Chem.* **1993**, *58* (27), 7865–7869.

(45) Vorm, S. van der; Hansen, T.; Overkleeft, H. S.; Marel, G. A. van der; Codée, J. D. C. The Influence of Acceptor Nucleophilicity on the Glycosylation Reaction Mechanism. *Chem. Sci.* **2017**, *8* (3), 1867–1875.

(46) Hagen, B.; Ali, S.; Overkleeft, H. S.; van der Marel, G. A.; Codée, J. D. C. Mapping the Reactivity and Selectivity of 2-Azidofucosyl Donors for the Assembly of *N*-Acetylfucosamine-Containing Bacterial Oligosaccharides. *J. Org. Chem.* **2017**, *82* (2), 848–868.

(47) Hosoya, T.; Takano, T.; Kosma, P.; Rosenau, T. Theoretical Foundation for the Presence of Oxacarbenium Ions in Chemical Glycoside Synthesis. *J. Org. Chem.* **2014**, *79* (17), 7889–7894.

(48) Hosoya, T.; Kosma, P.; Rosenau, T. Contact Ion Pairs and Solvent-Separated Ion Pairs from D-Mannopyranosyl and D-Glucopyranosyl Triflates. *Carbohydr. Res.* **2015**, *401*, 127–131.

(49) Hosoya, T.; Kosma, P.; Rosenau, T. Theoretical Study on the Effects of a 4,6-*O*-Diacetal Protecting Group on the Stability of Ion Pairs from D-Mannopyranosyl and D-Glucopyranosyl Triflates. *Carbohydr. Res.* **2015**, *411*, 64–69.

(50) Whitfield, D. M. DFT Studies of the Ionization of Alpha and Beta Glycopyranosyl Donors. *Carbohydr. Res.* **2007**, *342* (12–13), 1726–1740.

(51) Whitfield, D. M. Plausible Transition States for Glycosylation Reactions. *Carbohydr. Res.* **2012**, *356*, 180–190.
(52) Whitfield, D. M. In a Glycosylation Reaction How Does a Hydroxylic Nucleophile Find the Activated Anomeric Carbon? *Carbohydr. Res.* **2015**, *403*, 69–89.
(53) Satoh, H.; Nukada, T. Computational Chemistry on Chemical Glycosylations. *Trends in Glycoscience and Glycotechnology* **2014**, *26* (147), 11–27.
(54) Ardèvol, A.; Biarnés, X.; Planas, A.; Rovira, C. The Conformational Free-Energy Landscape of β-D-Mannopyranose: Evidence for a $^{1}S_{5} \rightarrow B_{2,5} \rightarrow {}^{O}S_{2}$ Catalytic Itinerary in β-Mannosidases. *J. Am. Chem. Soc.* **2010**, *132* (45), 16058–16065.
(55) Davies, G. J.; Planas, A.; Rovira, C. Conformational Analyses of the Reaction Coordinate of Glycosidases. *Acc. Chem. Res.* **2012**, *45* (2), 308–316.
(56) Crich, D.; Sharma, I. Is Donor–Acceptor Hydrogen Bonding Necessary for 4,6-*O*-Benzylidene-Directed β-Mannopyranosylation? Stereoselective Synthesis of β-*C*-Mannopyranosides and α-*C*-Glucopyranosides. *Org. Lett.* **2008**, *10* (21), 4731–4734.
(57) Martin, A.; Arda, A.; Désiré, J.; Martin-Mingot, A.; Probst, N.; Sinaÿ, P.; Jiménez-Barbero, J.; Thibaudeau, S.; Blériot, Y. Catching Elusive Glycosyl Cations in a Condensed Phase with HF/SbF_5 Superacid. *Nat. Chem.* **2016**, *8* (2), 186–191.
(58) Lebedel, L.; Ardá, A.; Martin, A.; Désiré, J.; Mingot, A.; Aufiero, M.; Aiguabella Font, N.; Gilmour, R.; Jiménez-Barbero, J.; Blériot, Y.; Thibaudeau, S. Structural and Computational Analysis of 2-Halogeno-Glycosyl Cations in the Presence of a Superacid: An Expansive Platform. *Angew. Chem. Int. Ed.* **2019**, *58* (39), 13758–13762.
(59) Elferink, H.; Severijnen, M. E.; Martens, J.; Mensink, R. A.; Berden, G.; Oomens, J.; Rutjes, F. P. J. T.; Rijs, A. M.; Boltje, T. J. Direct Experimental Characterization of Glycosyl Cations by Infrared Ion Spectroscopy. *J. Am. Chem. Soc.* **2018**, *140* (19), 6034–6038.
(60) Elferink, H.; Mensink, R. A.; Castelijns, W. W. A.; Jansen, O.; Bruekers, J. P. J.; Martens, J.; Oomens, J.; Rijs, A. M.; Boltje, T. J. The Glycosylation Mechanisms of 6,3-Uronic Acid Lactones. *Angew. Chem. Int. Ed.* **2019**, *58* (26), 8746–8751.
(61) Mucha, E.; Marianski, M.; Xu, F.-F.; Thomas, D. A.; Meijer, G.; von Helden, G.; Seeberger, P. H.; Pagel, K. Unravelling the Structure of Glycosyl Cations via Cold-Ion Infrared Spectroscopy. *Nat. Commun.* **2018**, *9* (1), 1–5.
(62) Huang, M.; Garrett, G. E.; Birlirakis, N.; Bohé, L.; Pratt, D. A.; Crich, D. Dissecting the Mechanisms of a Class of Chemical Glycosylation Using Primary ^{13}C Kinetic Isotope Effects. *Nat. Chem.* **2012**, *4* (8), 663–667.
(63) Crich, D.; Chandrasekera, N. S. Mechanism of 4,6-*O*-Benzylidene-Directed β-Mannosylation as Determined by α-Deuterium Kinetic Isotope Effects. *Angew. Chem.* **2004**, *116* (40), 5500–5503.
(64) Adero, P. O.; Furukawa, T.; Huang, M.; Mukherjee, D.; Retailleau, P.; Bohé, L.; Crich, D. Cation Clock Reactions for the Determination of Relative Reaction Kinetics in Glycosylation Reactions: Applications to Gluco- and Mannopyranosyl Sulfoxide and Trichloroacetimidate Type Donors. *J. Am. Chem. Soc.* **2015**.
(65) Huang, M.; Retailleau, P.; Bohé, L.; Crich, D. Cation Clock Permits Distinction Between the Mechanisms of α- and β-*O*- and β-*C*-Glycosylation in the Mannopyranose Series: Evidence for the Existence of a Mannopyranosyl Oxocarbenium Ion. *J. Am. Chem. Soc.* **2012**, *134* (36), 14746–14749.
(66) Vorm, S. van der; Hansen, T.; Hengst, J. M. A. van; S. Overkleeft, H.; Marel, G. A. van der; C. Codée, J. D. Acceptor Reactivity in Glycosylation Reactions. *Chem. Soc. Rev.* **2019**, *48* (17), 4688–4706.